ARTHRITIS & RHEUMATOLOGY
Vol. 69, No. 1, January 2017, pp 131–142
DOI 10.1002/art.39810

Tartrate-Resistant Acid Phosphatase Deficiency in the Predisposition to Systemic Lupus Erythematosus

Jie An,[1] Tracy A. Briggs,[2] Audrey Dumax-Vorzet,[3] Marta E. Alarcón-Riquelme,[4] Alexandre Belot,[5] Michael Beresford,[6] Ian N. Bruce,[7] Claudia Carvalho,[8] Laurence Chaperot,[9] Johan Frostegård,[10] Joel Plumas,[9] Gillian I. Rice,[3] Timothy J. Vyse,[11] Alice Wiedeman,[1] Yanick J. Crow,[12] and Keith B. Elkon[1]

Objective. **Mutations in the *ACP5* gene, which encodes tartrate-resistant acid phosphatase (TRAP), cause the immuno-osseous disorder spondyloenchondrodysplasia, which includes as disease features systemic lupus erythematosus (SLE) and a type I interferon (IFN) signature. Our aims were to identify TRAP substrates, determine the consequences of TRAP deficiency in immune cells, and assess whether *ACP5* mutations are enriched in sporadic cases of SLE.**

Methods. **Interaction between TRAP and its binding partners was tested by a yeast 2-hybrid screening, confocal microscopy, and immunoprecipitation/Western blotting. TRAP knockdown was performed using small interfering RNA. Phosphorylation of osteopontin (OPN) was analyzed by mass spectrometry. Nucleotide sequence analysis of *ACP5* was performed by Sanger sequencing or next-generation sequencing.**

Results. **TRAP and OPN colocalized and interacted in human macrophages and plasmacytoid dendritic cells (PDCs). TRAP dephosphorylated 3 serine residues on specific OPN peptides. TRAP knockdown resulted in increased OPN phosphorylation and increased nuclear translocation of *IRF7* and *P65*, with resultant heightened expression of IFN-stimulated genes and *IL6* and *TNF* following Toll-like receptor 9 stimulation. An excess of heterozygous *ACP5* missense variants was observed in SLE compared to controls ($P = 0.04$), and transfection experiments revealed a significant reduction in TRAP activity in a number of variants.**

The views expressed herein are those of the authors and not necessarily those of the NHS, the National Institute for Health Research, or the Department of Health.

Dr. An's work was supported by the Alliance for Lupus Research. Dr. Briggs' work was supported by the National Institute for Health Research (NIHR), a L'Oréal-UNESCO UK and Ireland Fellowship for Women in Science, and the NIHR Manchester Musculoskeletal Biomedical Research Unit. Dr. Dumax-Vorzet's work was supported by the Alliance for Lupus Research. Dr. Bruce's work was supported by Arthritis Research UK, the NIHR Manchester Biomedical Research Unit, and the NIHR/Wellcome Trust Manchester Clinical Research Facility; he is also an NIHR Senior Investigator. Dr. Crow's work was supported by the European Research Council (Fellowship GA 309449) and by a state subsidy managed by the National Research Agency (France) under the Investments for the Future program (grant ANR-10-IAHU-01).

[1]Jie An, PhD, Alice Wiedeman, PhD, Keith B. Elkon, MD: University of Washington, Seattle; [2]Tracy A. Briggs, MD, PhD: University of Manchester and St. Mary's Hospital, Central Manchester Foundation Trust, Manchester, UK; [3]Audrey Dumax-Vorzet, PhD (current address: Keele University, Staffordshire, UK), Gillian I. Rice, PhD: University of Manchester, Manchester, UK; [4]Marta E. Alarcón-Riquelme, MD, PhD: Universidad de Granada–Junta de Andalucía, Granada, Spain, and Oklahoma Medical Research Foundation, Oklahoma City; [5]Alexandre Belot, MD, PhD: Pediatric Rheumatology Unit, Femme Mère Enfant Hospital, Hospices Civils de Lyon, INSERM U1111, University of Lyon, Lyon, France; [6]Michael Beresford, MD, PhD: Institute of Translational Medicine, University of Liverpool, Liverpool, UK; [7]Ian N. Bruce, MD: University of Manchester and Central Manchester University Hospitals NHS Foundation Trust, Manchester, UK; [8]Claudia Carvalho, MSc: Universidade do Porto, Abel Salazar Institute of Biomedical Sciences, Porto, Portugal; [9]Laurence Chaperot, PhD, Joel Plumas, PhD: INSERM U823/UJF/EFS, UGA, INSERM U1209, CNRS 5309, Immunobiology and Immunotherapy of Cancers and Chronic Diseases, Grenoble, France; [10]Johan Frostegård, MD, PhD: Karolinska Institutet, Stockholm, Sweden; [11]Timothy J. Vyse, MD, PhD: King's College London, Guy's Hospital, London, UK; [12]Yanick J. Crow, MD, PhD: University of Manchester, Manchester, UK, and Institut Imagine, Laboratory of Neurogenetics and Neuroinflammation, Paris, France.

Drs. An and Briggs contributed equally to this work.

Address correspondence to Tracy A. Briggs, MD, PhD, Genomic Medicine, Manchester Academic Heath Science Centre, St. Mary's Hospital, Central Manchester Foundation Trust, Oxford Road, Manchester M13 9WL, UK (e-mail: tracy.briggs@manchester.ac.uk); or to Keith B. Elkon, MD, University of Washington, Division of Rheumatology, 1959 NE Pacific Street, Seattle, WA 98195 (e-mail: kelkon@medicine.washington.edu).

Submitted for publication August 9, 2015; accepted in revised form June 30, 2016.

Conclusion. **Our findings indicate that TRAP and OPN colocalize and that OPN is a substrate for TRAP in human immune cells. TRAP deficiency in PDCs leads to increased IFNα production, providing at least a partial explanation for how *ACP5* mutations cause lupus in the context of spondyloenchondrodysplasia. Detection of *ACP5* missense variants in a lupus cohort suggests that impaired TRAP functioning may increase susceptibility to sporadic lupus.**

Tartrate-resistant acid phosphatase (TRAP) is a member of the purple acid phosphatase family and is also referred to as type 5 acid phosphatase. It is predominantly expressed in cells of monocytic lineage, including osteoclasts, macrophages, and dendritic cells (DCs) (1–3). There are 2 isoforms of the TRAP enzyme: TRAP-5a and TRAP-5b, with TRAP-5b being produced by posttranslational modification of TRAP-5a. TRAP-5b is the major isoform of TRAP secreted by osteoclasts, and TRAP-5b activity has been shown to correlate with osteoclast number and activity in the serum, both in rat and in human studies (4–6). In contrast, macrophages and DCs are believed to secrete TRAP-5a as the predominant isoform, and TRAP-5a is a nonspecific marker for macrophage activation (7,8). Most studies of TRAP function relate to its role in the osteoclast, where extracellular TRAP has been strongly implicated in the regulation of osteoclast attachment and migration, particularly via the dephosphorylation of osteoclast-secreted osteopontin (OPN) (9). OPN is a highly phosphorylated, multifunctional glycoprotein that is secreted into biologic fluids by many cell types, including osteoclasts, macrophages, and T cells (10). OPN is known to be a key protein in bone mineralization, and it is thought that phosphorylated OPN facilitates attachment of the osteoclast to the resorbing bone matrix. Consequently, OPN dephosphorylated by secreted TRAP leads to osteoclast release and migration (9).

We and other investigators have previously reported that biallelic mutations in the gene *ACP5*, which encodes TRAP, result in spondyloenchondrodysplasia (SPENCD), a rare pediatric disorder (11,12). Patients with SPENCD demonstrate a skeletal dysplasia reminiscent of that observed in the ACP5-knockout mouse (13). Interestingly, however, patients also manifest a variable neurologic and autoimmune phenotype. These autoimmune features include antinuclear antibody (ANA) and anti–double-stranded DNA (anti-dsDNA) antibody, autoimmune thrombocytopenic purpura, and systemic lupus erythematosus (SLE). Patients with SPENCD consistently show an overexpression of interferon (IFN)–stimulated genes (ISGs) in whole blood, which is an IFN signature, although the link from TRAP deficiency to IFN signaling remains unexplained.

Initial studies have implicated OPN as being potentially relevant to the pathology of SPENCD (11,12). OPN, also known as early T lymphocyte activation I (14), is reported to be involved in diverse immune processes, such as macrophage activation, inflammation, and leukocyte recruitment, many of which are phosphorylation-dependent. It also plays a critical role in the efficient development of Th1 immune responses in T cells. Of note, polymorphisms in *OPN* and increased serum levels of OPN have been associated with elevated IFNα levels in individuals with SLE (15). In the mouse, OPN has been shown to be integral to IFNα production in plasmacytoid dendritic cells (PDCs), a major source of type I IFN (16).

Studies to date have highlighted SPENCD as a rare Mendelian cause of lupus and suggest an association between TRAP, OPN, and IFN metabolism. The aim of our research was to decipher the detailed cellular pathways linking these molecules and to understand how a loss of TRAP activity predisposes to autoimmune disease, particularly SLE.

MATERIALS AND METHODS

Confocal microscopy. A Gen 2.2 PDC line was stained for immunofluorescence microscopy following adherence on polylysine slides. Macrophage colony-stimulating factor–derived human macrophages prepared from CD14+ circulating precursors were stained for immunofluorescence analysis in 4-chamber slides on day 5 (plated at 500,000 cells/ml per chamber on day 0). TRAP, OPN, IFN regulatory factor 7 (IRF-7), and NF-κB were detected with anti–TRAP-5a rabbit sera (17), mouse monoclonal anti-OPN antibody (Novus Biologicals), rabbit polyclonal anti–IRF-7, and anti-p65 (Santa Cruz Biotechnology), respectively, followed by fluorescein isothiocyanate–labeled donkey anti-rabbit IgG (for TRAP, IRF-7, and p65) and AF-555 donkey anti-mouse IgG (for OPN) secondary antibodies. Nuclei were stained with DAPI. Stained cells were viewed with a Zeiss LSM 510 confocal microscope with a 1.4 numerical aperture 63× oil immersion lens. The images were analyzed with ImageJ software (National Institutes of Health). Three focal planes were analyzed, with ~20 cells in each focal plane, derived from 2 independent experiments. Nuclear translocation was quantified as the ratio of the intensity of the IRF-7/NF-κB signal within the DAPI-positive nucleus to that in the cytoplasm.

RNA and complementary DNA (cDNA) preparation and quantitative real-time polymerase chain reaction (PCR). Total RNA was isolated from PDCs using an RNeasy mini kit (Qiagen). We synthesized cDNA using 100 ng of RNA with a high-capacity cDNA reverse transcription kit with random primers (Applied Biosystems). Reactions were performed in duplicate and were run on an ABI StepOnePlus system using primers for *18S*, *ACP5*, *CXCL10*, *IFI27*, *IFI44L*, *MX1*, and *PKR* (Supplementary Table 1, available on the *Arthritis & Rheumatology* web site at http://onlinelibrary.wiley.com/doi/10.1002/art.39810/abstract). A 2-stage cycle of 95°C for 15 seconds and 60°C for 1 minute was repeated for 40 cycles, followed by a dissociation stage. Threshold cycle values were set as a constant at 0.2, and

fold changes in gene expression were then calculated using the $2^{-\Delta\Delta C_t}$ method.

Western blotting. Cells were lysed in lysis buffer composed of 0.5% Nonidet P40 in 1× Tris buffered saline–Tween, and 20 μg of protein from each sample was loaded onto sodium dodecyl sulfate–polyacrylamide gel electrophoresis gels for Western blotting. Anti-TRAP (USB) and anti-OPN (R&D Systems) antibodies were used at a dilution of 1:1,000. Signals were detected with an ECL detection system and film (GE Healthcare). A Bio-Rad imaging system was used for quantification, with normalization against the intensity of β-actin. Quantitative infrared Western blotting was carried out with lysates of HEK 293 cells that had been transiently transfected with different homozygous *ACP5* variants, using primary mouse antihemagglutinin (anti-HA; Sigma-Aldrich) and rabbit antitubulin (Sigma) antibodies, with secondary IRDye 800CW goat anti-mouse IgG and IRDye 680RD goat anti-rabbit IgG (both from Li-Cor) antibodies. Rather than TRAP antibody, we used HA-tag antibody to exclude potential interference of point mutations with epitope recognition. Quantification of bands was performed using Odyssey analysis software (Li-Cor).

Yeast 2-hybrid screen. A yeast 2-hybrid screen was performed by Hybrigenics services (www.hybrigenics-services.com) using an N-LexA-ACP5-C fusion protein and an N-Gal4-ACP5-C fusion protein on a human macrophage cDNA library from monocyte-derived macrophages obtained from healthy donors. The N-Gal4-ACP5-C fusion yielded 36 positive clones, which were assessed for interactions and categorized as A–E according to predicted confidence in results, with A indicating the highest degree of confidence in the interaction.

Generation of PDC and THP-1 TRAP-knockdown cell lines. The Gen 2.2 PDC line or THP-1 cells were transfected with TRAP-5 or nontarget short hairpin RNA (shRNA) control Mission shRNA lentiviral transduction particles (Sigma) according to the manufacturer's instructions. The stable PDC lines or THP-1 cell lines with *TRAP5*-specific shRNA or scrambled shRNA were established after puromycin selection. The knockdown of *TRAP* was confirmed by quantitative PCR with *ACP5*-specific primers (Supplementary Table 1).

Phosphorylation analysis by mass spectrometry. TRAP-knockdown THP-1 cells were differentiated into macrophage-like cells by overnight stimulation with phorbol myristate acetate (20 n*M*). Cells were lysed with 6*M* urea in 50 m*M* ammonium bicarbonate. Proteins from cell lysate or recombinant OPN were reduced with tris(2-carboxyethyl)phosphine for 1 hour at 37°C and alkylated with iodoacetamide for 1 hour at room temperature in the dark. Proteins were digested overnight at 37°C with trypsin at a 1:50 enzyme-to-protein ratio. The peptides were then washed 3 times and desalted in C18 columns. Phosphopeptides were enriched in a TiO_2 column and desalted in graphite columns according to the manufacturer's instructions. Phosphopeptides from recombinant OPN (R&D Systems) were analyzed by ultra-performance liquid chromatography (UPLC; Waters) coupled with LTQ Orbitrap mass spectrometry (Thermo Scientific). Phosphopeptides from cell lysates were analyzed by UPLC coupled with Orbitrap fusion mass spectrometry (Thermo Scientific).

Subjects. DNA samples were collected from patients with confirmed lupus, as defined by the American College of Rheumatology (ACR) criteria (18) and from controls. A total of 975 samples were obtained from adult lupus patients: 240 Swedish, 162 Portuguese, 352 British, and 92 Argentinian, as well as 129 British pediatric lupus patients. A total of 529 control samples were obtained from adult subjects: 92 Swedish, 189 Portuguese, 61 British, and 187 mixed European individuals. Patients and control populations were matched in terms of ethnicity for all samples except for the 92 samples from the Argentinian lupus patients and the 187 samples from the mixed European controls. Appropriate consents for study and ethics approvals were obtained for each research group from which samples were obtained.

Sequence analysis. Sanger sequencing was undertaken in 890 lupus patients and all controls. PCR amplification of all coding exons of *ACP5* was performed (sequences available upon request from the corresponding author). Purified PCR amplification products were sequenced using dye-terminator chemistry and electrophoresed on an ABI 3130 capillary sequencer. As genetic techniques evolved over time, targeted enrichment and sequencing were subsequently undertaken in 85 patients with pediatric SLE. Enrichment was undertaken using SureSelect Human All Exon kits (Agilent) according to the manufacturer's protocol, and samples were paired-end sequenced on an Illumina HiSeq 2000 platform. Sequence data were mapped using the Burrows-Wheeler aligner and the hg18 (NCBI36) human genome as a reference. Data from 200 selected candidate lupus genes, including *ACP5*, were extracted. Variants were called using the Short Oligonucleotide Analysis software package, with medium stringency. Variants were confirmed by Sanger sequencing.

The mutation description is based on the reference cDNA sequence NM_001111035, with the ATG initiation site situated at the beginning of exon 4 and the termination codon in exon 7. The pathogenicity of variants was analyzed using Alamut, SIFT, and PolyPhen and in the context of the crystal structure (19). Minor allele frequency was assessed using the Exome Aggregation Consortium (ExAC) database (http://exac.broadinstitute.org).

Transient constructs. Wild-type (WT) human *ACP5* cDNA coupled to an in-frame Strep-tag or HA-tag was cloned into pcDNA3.2/GW/V5/D-TOPO vector (Invitrogen), and site-directed mutagenesis was performed to introduce individual point mutations into the *ACP5*–HA followed by confirmatory Sanger sequencing. The pcDNA3.2/GW/V5/D-TOPO without any *ACP5* cDNA insert (empty vector) was used as a control. HEK 293 cells were transfected overnight with 4 μg of plasmid DNA using 10 μl of Lipofectamine 2000 (ThermoFisher Scientific) according to the manufacturer's instructions. In preliminary studies, we verified that monomeric and cleaved TRAP were both detected in cell lysates, whereas only monomeric TRAP was detected in supernatant, using an anti-TRAP antibody and Western blotting. In addition, glycosylation appeared similar between WT and mutant protein, as determined by endoglycosidase H and peptide *N*-glycanase F sensitivity (data not shown).

TRAP activity. A Biomol Green assay was undertaken by incubating 1 μg of recombinant human TRAP and 1 μg of recombinant human or bovine milk OPN together in 0.4*M* sodium acetate and 200 m*M* sodium tartrate buffer (pH 5.6) overnight at 37°C. The free phosphate released from OPN was measured according to the manufacturer's instructions (Enzo Life Sciences). Phosphate standards (serial dilution from 2 nmoles to 0.031 nmoles) were used for the standard curve to quantify the released free phosphate. A paranitrophenyl phosphate (PNPP) assay was performed as previously described

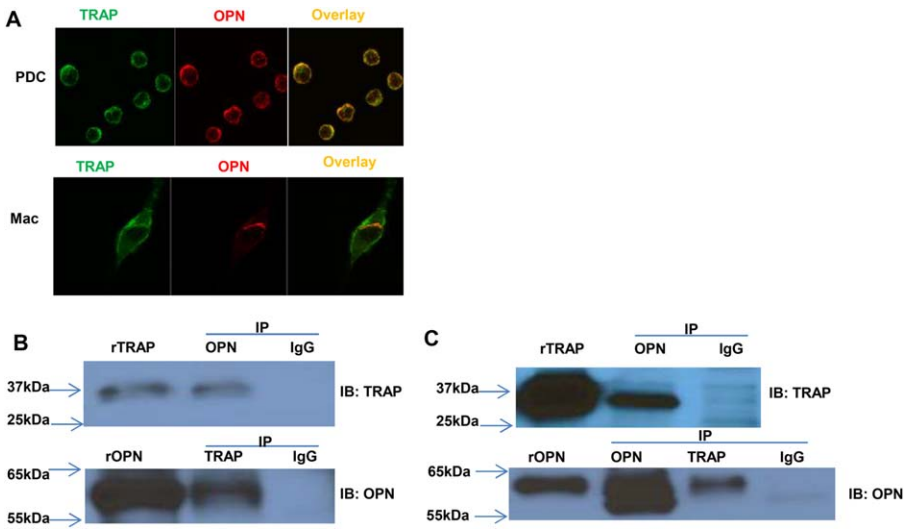

Figure 1. Colocalization and interaction of tartrate-resistant acid phosphatase (TRAP) and osteopontin (OPN) in plasmacytoid dendritic cells (PDCs) and primary human macrophages. **A,** Confocal microscopy of TRAP (green) and OPN (red) with the overlay demonstrating partial colocalization in the PDC line Gen 2.2 (top) and in macrophages (Mac) (bottom). Images are representative of 4 independent experiments. Images were obtained using a 63× oil objective. **B,** Interaction of TRAP with OPN. HEK 293 cells were cotransfected with OPN and TRAP, and after 48 hours, cells were lysed and target proteins immunoprecipitated (IP) with antibodies to the indicated antigens. Samples were resolved by sodium dodecyl sulfate–polyacrylamide gel electrophoresis, and immunoblotting (IB) was performed with antibodies to the indicated antigens. Anti-OPN IP followed by anti-TRAP IB is shown at the top and anti-TRAP IP followed by anti-OPN IB at the bottom. Recombinant human TRAP (rTRAP) and recombinant human OPN (rOPN) were used as positive controls and IgG as isotype control. **C,** Immunoprecipitation and immunoblotting as in **B**, using lysates prepared from primary macrophages stimulated for 18 hours with CpG-B. Anti-OPN IP followed by anti-TRAP IB is shown at the top and anti-TRAP IP followed by anti-OPN at the bottom. Results in **B** and **C** are from 2 independent experiments.

(17,20). The concentration of paranitrophenol was normalized using the protein concentration in the cell lysate. TRAP immunocytochemistry was undertaken by the addition of naphthol AS-Bl phosphoric acid (Sigma-Aldrich), which hydrolyzed to naphthol AS-BI in the presence of TRAP and coupled with fast garnet GBC to form insoluble maroon deposits at the site of activity.

Statistical analysis. Statistical significance between groups was determined by unpaired/paired *t*-test or chi-square test where appropriate. Correlations between parameters were assessed using the Pearson correlation analysis and linear regression analysis. Graphs and statistical analyses were performed using GraphPad Prism software version 4.

RESULTS

TRAP colocalization and physical interaction with OPN in PDCs and macrophages. Since OPN is a substrate for TRAP in osteoclasts (21), we wanted to determine whether this was also the case in macrophages and PDCs. As shown in Figure 1A, OPN and TRAP colocalized both in the unstimulated human PDC line Gen 2.2 (22) (hereinafter referred to as PDC line) and in human primary monocyte-derived macrophages, as determined by confocal microscopy. We performed organelle studies and determined that both OPN and TRAP were localized in the Golgi apparatus (Supplementary Figure 1, available online at http://onlinelibrary.wiley.com/doi/10.1002/art.39810/abstract).

To examine whether OPN and TRAP interact physically, we performed a yeast 2-hybrid screen in a human macrophage cDNA library. While no category A–C (high confidence) interacting partners of TRAP were identified, 6 category D (moderate confidence) interacting partners were demonstrated, including OPN, conserved oligomeric Golgi 1 (a Golgi-processing protein), upstream stimulatory factor 2 (a transcription factor that is postulated to play a functional role in RANKL-dependent TRAP expression during osteoclast differentiation [23]), and 3 genes of unknown name or function. To confirm OPN as an interacting partner, we overexpressed OPN and TRAP in HEK 293 cells (Supplementary Figure 2, available online at http://onlinelibrary.wiley.com/doi/10.1002/art.39810/abstract) and performed immunoblot analysis (Figure 1B). TRAP was coprecipitated when OPN was immunoprecipitated, while in the reciprocal experiment, OPN was coprecipitated with TRAP. To verify that this interaction occurred in primary cells, we observed that when OPN was immunoprecipitated in monocyte-derived macrophages, TRAP was readily detected on the Western blot (Figure 1C). In the reciprocal experiment, OPN was coprecipitated with TRAP. Since the signal obtained with

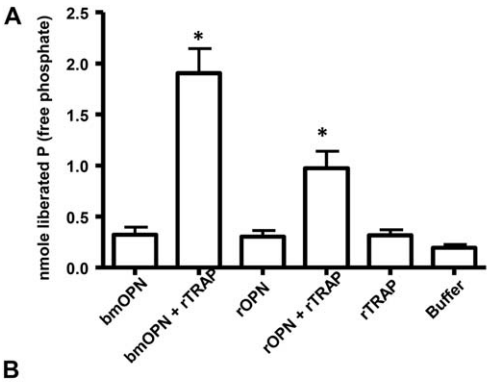

B

Sample No.	Protein probability	Protein Description	Peptide sequence
rOPN Only	1	Osteopontin	GKD*Sp*YETSQLDDQ*Sp*AETHSHK
rOPN Only	1	Osteopontin	ISHELD*Sp*ASpSEVN
rOPN + rTRAP	1	Osteopontin	GKD*S*YETSQLDDQ*S*AETHSHK
rOPN + rTRAP	1	Osteopontin	ISHELD*S*ASpSEVN

Figure 2. OPN as a substrate for TRAP. **A,** Measurement of free phosphate. Bovine milk OPN (bmOPN; 1 μg) or rOPN (1 μg) was incubated overnight in the presence or absence of rTRAP (1 μg) using methods described elsewhere (32). Free phosphates were quantified in a Biomol Green assay using phosphate as standards, with bmOPN, rOPN, rTRAP, and reaction buffer alone as negative controls for background signal. Values are the mean ± SEM. $* = P < 0.05$ versus the corresponding bmOPN and rOPN without rTRAP. **B,** Detection of peptides phosphorylated from OPN protein. Human rOPN (500 ng) was incubated overnight either alone or with rTRAP (500 ng). The reaction mixtures were trypsin digested and subjected to liquid chromatography tandem mass spectrometry to identify phosphorylated peptides. The 3 phosphorylation sites (phosphorylated serine [Sp]) on 2 peptides of OPN (top 2 rows) that were found to be dephosphorylated by TRAP (serine [S]) (bottom 2 rows) are shown in italics. Reactions in **A** and **B** were performed in duplicate. See Figure 1 for other definitions. Color figure can be viewed in the online issue, which is available at http://onlinelibrary.wiley.com/doi/10.1002/art.39810/abstract.

anti-OPN was much stronger than that precipitated by anti-TRAP (Figure 1C), these results suggest that only some of the OPN is associated with TRAP. In summary, the yeast 2-hybrid and coprecipitation data, together with the findings of the confocal studies, indicated that OPN and TRAP interact with each other and that OPN is a substrate for TRAP in some human immune cells.

OPN as a substrate of TRAP in vitro. OPN has the potential to be extensively modified by alteration of its phosphorylation state, as there are a number of serine/threonine phosphorylation sites distributed throughout the protein. The degree of phosphorylation varies depending upon the source of the OPN. For example, human and bovine milk OPN contain 32 and 28 serine/threonine phosphorylation sites, respectively. The degree of phosphorylation of other forms of OPN, such as recombinant OPN, is less certain (24,25). To assess whether human OPN is a substrate for TRAP, recombinant human OPN (rOPN) was incubated with recombinant human TRAP (rTRAP), and the amount of free/liberated phosphate was measured with the Biomol Green assay. Phosphate release significantly increased when rOPN and rTRAP were incubated together, as was also seen in the combined bovine milk OPN and rTRAP-positive control, as compared to other single-buffer controls (Figure 2A). To determine the residues at which TRAP removed phosphates, we performed UPLC–LTQ Orbitrap mass spectrometry of rOPN following incubation with rTRAP. Protein database search results revealed that TRAP consistently dephosphorylated 2 phosphoserine residues (Sp) in the peptide GKDSpYETSQLDDQSpAETHSHK and the first Sp in the peptide ISHELDSpASpSEVN (Figure 2B).

Increased IFNα, interleukin-6 (IL-6), and tumor necrosis factor (TNF) production in association with increased nuclear translocation of *IRF7* and *NFKB* following TRAP knockdown. Activation of Toll-like receptor 9 (TLR-9) in PDCs leads to nuclear translocation of *IRF7* and *NFKB*, resulting in the transcription of *IFNA*, *IL6*, and *TNF* (26). Since OPN was reported to associate with the TLR-9/MyD88 signaling complex in PDCs in mice (16) and since we have shown that TRAP can associate with OPN and dephosphorylate it, we investigated the effects of shRNA-mediated knockdown of TRAP in the PDC line. We established 3 PDC lines with stable knockdown of TRAP compared to empty vector and scrambled shRNA controls, both in unstimulated (average 67% knockdown) (Figure 3A) and in stimulated PDCs (average 75% knockdown) (Figure 3B). Consistent with a role of TRAP in the regulation of OPN function, a significant increase in the IFNα concentration was observed in the TRAP-knockdown PDC lines as compared to scrambled shRNA (control) following TLR-9 stimulation with CpG-A (Figure 3C). Consistent with the increase in IFNα concentration, expression of the ISGs *IFI27*, *CXCL10*, *IFI44L*, *PKR*, and *MX1* was increased in the TRAP-knockdown PDC line (Figure 3D). Of interest, stimulation of the TRAP knockdown PDC line with CpG-B also led to increased production of the cytokines TNF (Figure 3E) and IL-6 (Figure 3F).

To gain further insight into the mechanisms responsible for increased cytokine production, we examined the nuclear localization of the transcription factors IRF-7 and NF-κB, which are downstream of TLR-9, in PDCs. Whereas there was no difference in the localization of IRF-7 and NF-κB in unstimulated cells (Supplementary Figure 3, available online at http://onlinelibrary.wiley.com/doi/10.1002/art.39810/abstract), we observed significantly more IRF-7 (Figure 4A) and NF-κB (Figure 4B) nuclear translocation in the TRAP-knockdown PDC line as compared to the control PDC line following CpG

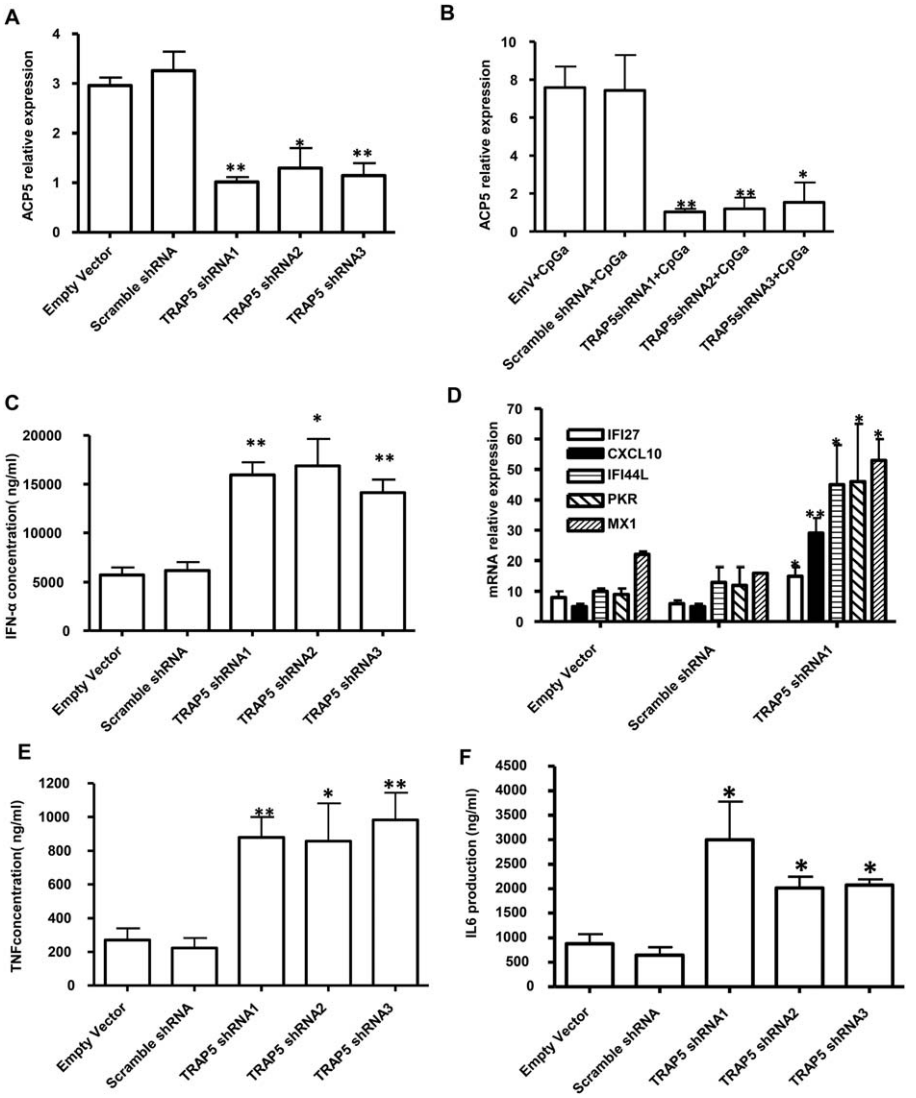

Figure 3. Increased production of interferon-α (IFNα), IFN-stimulated genes, tumor necrosis factor (TNF), and interleukin-6 (IL-6) in plasmacytoid dendritic cells (PDCs) following knockdown of tartrate-resistant acid phosphatase (TRAP). The Gen 2.2 PDC line was transfected with empty vector, scrambled short hairpin RNA (shRNA), or TRAP-5 shRNA (3 different clones) and was left unstimulated (**A**) or was stimulated for 16 hours with CpG-A (**B–D**) or CpG-B (**E** and **F**). **A** and **B,** Expression of mRNA for *ACP5*, as determined by quantitative polymerase chain reaction (qPCR) analysis. Results were normalized to the *18S* housekeeping gene. **C,** Production of IFNα cytokine, as determined by enzyme-linked immunosorbent assay (ELISA). **D,** Expression of mRNA for the IFN-stimulated genes *IFI27*, *CXCL10*, *IFI44L*, *PKR*, and *MX1*, as determined by qPCR analysis. Results were normalized to the *18S* housekeeping gene. **E** and **F,** Production of TNF (**E**) and IL-6 (**F**) cytokines, as quantified by ELISA. Values are the mean ± SEM of 6 independent experiments. $* = P < 0.05$; $** = P < 0.01$ versus scrambled shRNA.

stimulation. These data demonstrate that TRAP plays a role in the regulation of IFNα, IL-6, and TNF cytokine production in human PDCs. Consistent with the in vitro data, a number of SPENCD patients showed significant elevation of IL-6, but not TNF, expression in whole blood (Supplementary Figure 4, available online at http://onlinelibrary.wiley.com/doi/10.1002/art.39810/abstract), in addition to the elevated IFNα data reported previously (11).

Hyperphosphorylated OPN in TRAP-knockdown versus control THP-1 cells. To further verify that TRAP regulates OPN function in PDCs, we determined whether there was differential phosphorylation of OPN in TRAP-knockdown versus control PDCs. Due to the low expression of OPN in the PDC line, attempts to detect phosphopeptides following CpG stimulation were unsuccessful. We therefore examined a TRAP-knockdown THP-1 cell line. Following phorbol myristate acetate stimulation and

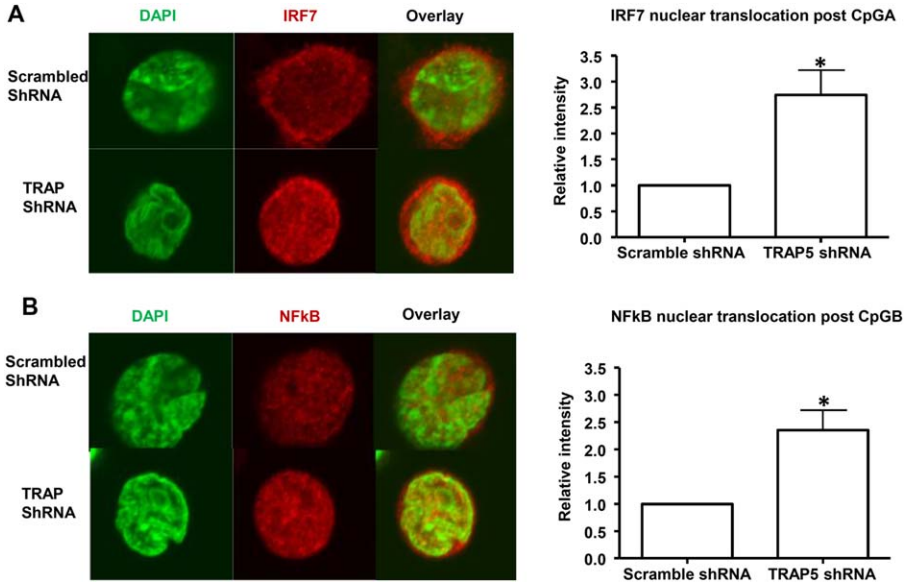

Figure 4. Increased nuclear translocation of interferon regulatory factor 7 (IRF-7) and NF-κB in plasmacytoid dendritic cells (PDCs) following knockdown of tartrate-resistant acid phosphatase (TRAP). Nuclear translocation of IRF-7 (stimulated with CpG-A) (**A**) and NF-κB p65 subunit (stimulated with CpG-B) (**B**) was examined following TRAP knockdown with short hairpin RNA (shRNA) or scrambled shRNA (control) in the Gen 2.2 PDC line. Cells were stimulated with CpG for 1 hour and examined by confocal microscopy using DAPI (pseudogreen) to stain the nucleus and an antibody to the transcription factor IRF-7 or the p65 subunit of NF-κB, respectively (pseudored). Representative images are shown at the left. Images were obtained using a 63× oil objective. Relative intensity of IRF-7 and NF-κB nuclear translocation in TRAP-knockdown PDCs versus scrambled shRNA controls, as quantified using ImageJ software, is shown at the right. Values are the mean ± SEM of 2 independent experiments. $* = P < 0.05$.

differentiation to macrophage-like cells, TRAP-knockdown THP-1 cells consistently demonstrated an increased amount of hyperphosphorylated OPN compared to controls, as quantified by liquid chromatography tandem mass spectrometry (LC-MS/MS) (Figure 5A). The hyperphosphorylated sites were within the same 2 peptides identified with rOPN (Figure 2B), and 2 of the 3 phosphorylated sites were the same (Figures 5B and C). Hyperphosphorylation of OPN in TRAP-knockdown cells further indicated that OPN is a substrate for TRAP in human immune cells and that TRAP regulation of OPN by dephosphorylation may regulate IFN production (Figure 5D).

***ACP5* heterozygous variants in SLE.** In view of the high prevalence of lupus in patients with SPENCD (11,27), we sought to determine whether TRAP influenced susceptibility to idiopathic SLE. To address this question, we sequenced all coding exons of the *ACP5* gene in 890 SLE patients and 529 healthy controls by the Sanger method, and a further 85 pediatric SLE patients underwent next-generation sequencing. Patient and control populations were matched in terms of ethnicity, except for the 92 samples from the Argentinian lupus patients and the 187 samples from the mixed European controls. An analysis of Hardy-Weinberg equilibrium and the frequency of 3 commonly occurring SNPs suggested that all groups were directly comparable. We assessed for rare, nonsynonymous variants or canonical intronic variants within the cohorts, as these were considered more likely to be of functional effect. We defined rare as a minor allele frequency (MAF) of <0.002 in the ExAC database, which includes data on *ACP5* on ~120,000 control population alleles. An MAF of <0.002 was chosen because this is the MAF of the most common disease-causing variant observed in the Mendelian interferonopathy Aicardi-Goutières syndrome (P193A mutation in *ADAR1*) (28). This variant has unequivocal pathogenicity, and we therefore considered that variants up to this MAF cutoff may be disease-causing.

We observed an increased number of rare heterozygous missense *ACP5* variants in the SLE patients (15 of 975) compared to controls (2 of 529) ($P = 0.044$). There was a total of 13 different rare variants in a total of 12 adults and 3 children that were distributed across the ethnic groups assessed (5 British, 4 Swedish, 4 Portuguese, and 2 Argentinian). When in silico testing was performed, the missense residues were moderately conserved to well conserved in mammalian species, and the majority were predicted to destabilize the protein on in silico modeling (Supplementary Table 2, available online

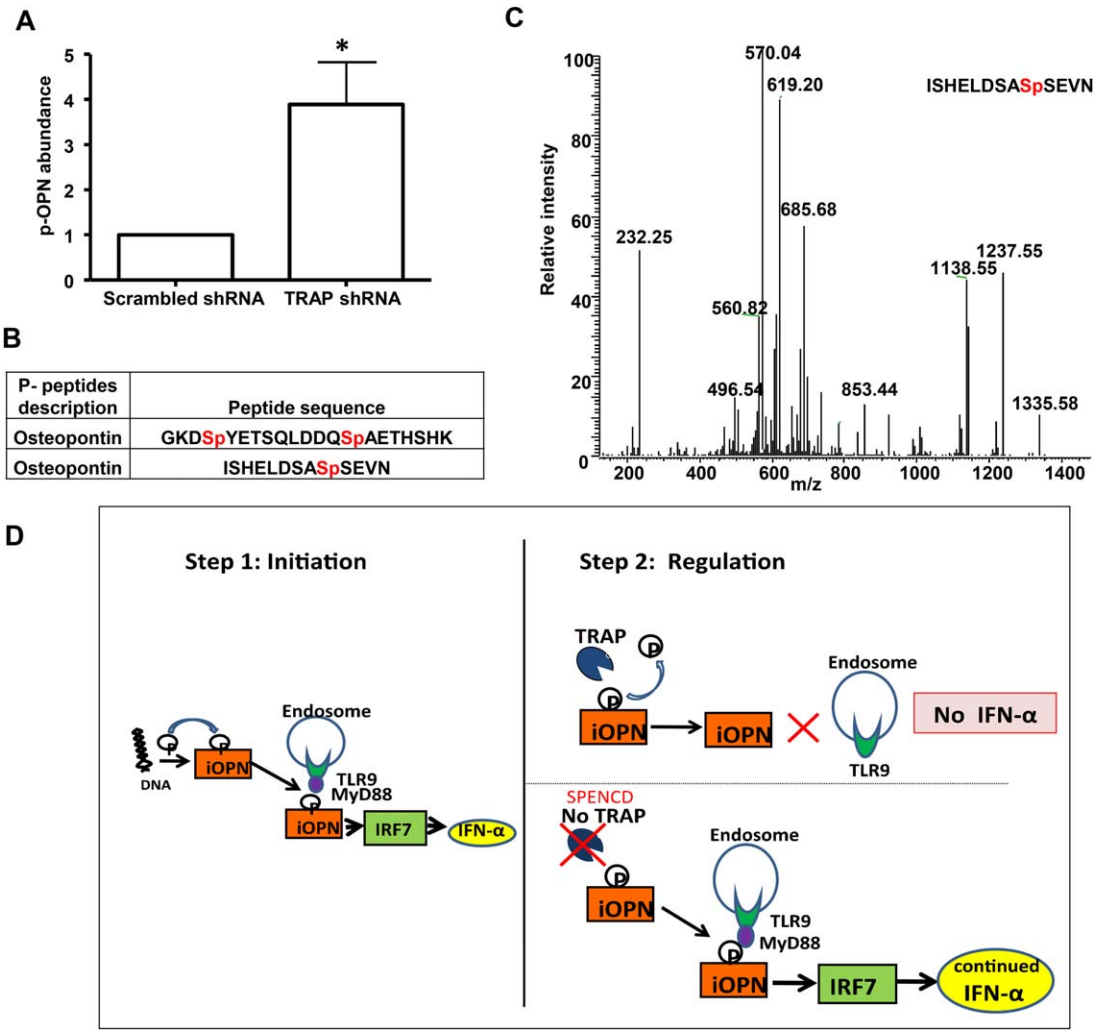

Figure 5. Hyperphosphorylation of osteopontin (OPN) in THP-1 cells following tartrate-resistant acid phosphatase (TRAP) knockdown. THP-1 cells were transfected with scrambled short hairpin RNA (shRNA; control) or TRAP shRNA and differentiated to macrophage-like cells with phorbol myristate acetate. Phosphopeptides were prepared for liquid chromatography tandem mass spectrometry (see Materials and Methods). Acquired OPN phosphopeptide counts were normalized to total peptide counts in the same mass spectrometry run for the quantification of OPN phosphopeptides in scrambled shRNA and TRAP shRNA samples. **A,** Comparison of phosphorylated OPN (p-OPN) peptides in cells following scrambled shRNA versus TRAP shRNA knockdown. Values are the mean ± SEM. $* = P < 0.05$. **B,** The 3 serine residues in 2 peptides of OPN that were found to be hyperphosphorylated by TRAP shRNA (hyperphosphorylated serine [Sp]) (shown in red). Results are from 4 independent experiments. **C,** Representative results of the mass spectrum of the phosphopeptide: ISHELDSASpSEVN. Values are the mass-to-charge ratio (m/z) of the fragmented ions from the peptides. **D,** Model of the TRAP/OPN axis in the regulation of interferon-α (IFNα). Step 1 illustrates phosphorylation, and thus activation, of intracellular OPN (iOPN), perhaps by a DNA ligand. Activated iOPN then forms a complex with Toll-like receptor 9 (TLR-9) and myeloid differentiation factor 88 (MyD88) and, via IFN regulatory factor 7 (IRF-7), induces IFNα production. Step 2 (top) shows regulation of the pathway, which is achieved by dephosphorylation of OPN by TRAP, with subsequent inhibition of IFNα induction. With the continued formation of the iOPN/MyD88/TLR-9 signalosome (step 2, bottom), there is prolonged IFNα production due to a TRAP deficiency, as in spondyloenchondrodysplasia (SPENCD) and possibly in some cases of systemic lupus erythematosus. P = free phosphate.

at http://onlinelibrary.wiley.com/doi/10.1002/art.39810/abstract). One of the variants, $Met^{264}Lys$, has previously been reported in the homozygous state in a patient with SPENCD (11).

To test whether the *ACP5*-heterozygous variants identified in the SLE cohort could cause a reduction in TRAP activity, we produced HEK 293 cells expressing homozygous *ACP5* constructs and, subsequently, cotransfections of wild-type and variant constructs. In the lysate and supernatant of cells transiently transfected with 11 different homozygous variant constructs, a significant reduction of TRAP activity (assessed by the PNPP assay) was

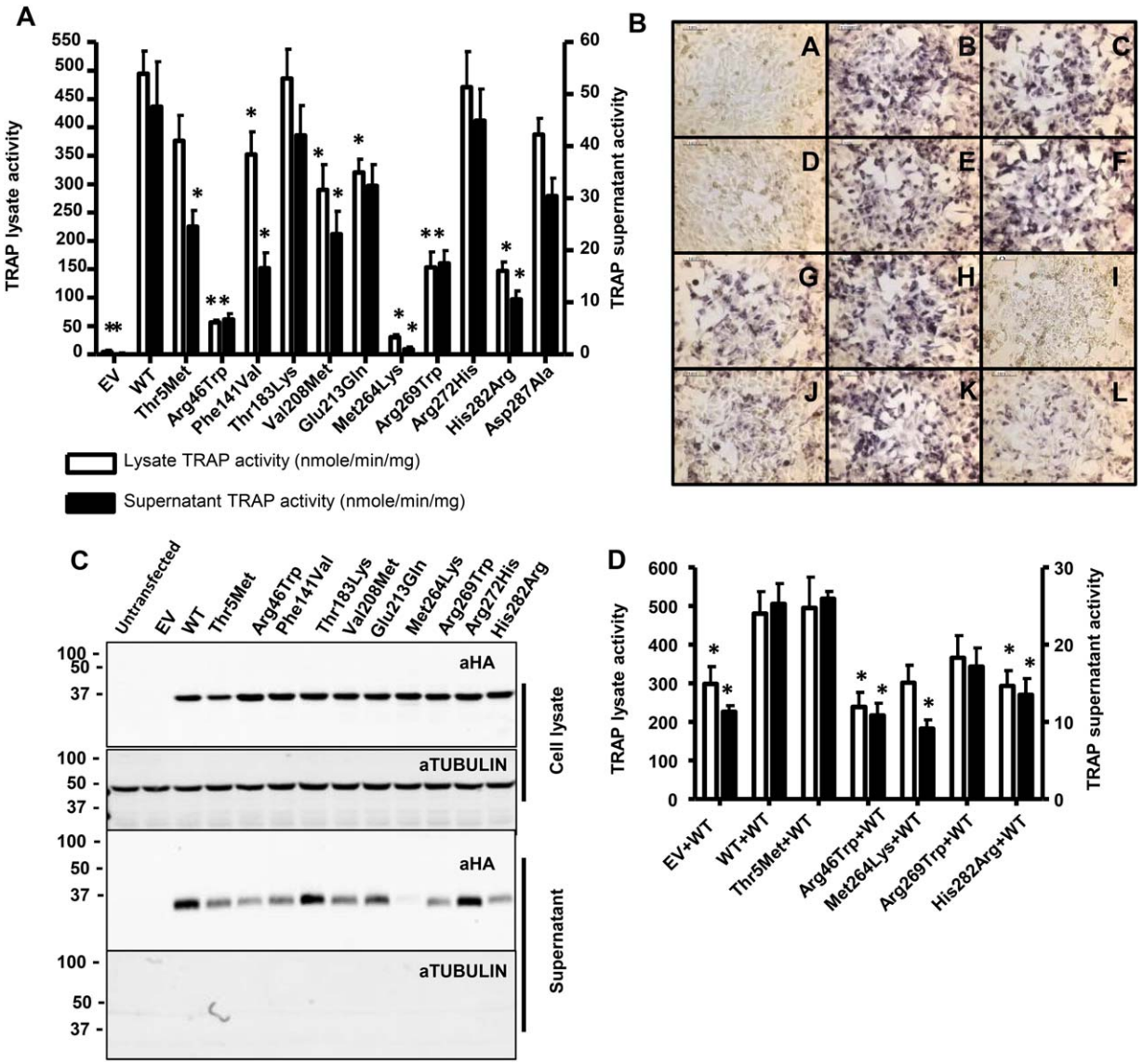

Figure 6. Tartrate-resistant acid phosphatase (TRAP) activity in HEK 293 cells transiently transfected with homozygous or heterozygous *ACP5* variants identified in a lupus cohort. **A,** Paranitrophenyl phosphate (PNPP) activity in cell lysates and supernatants of 11 homozygote variant constructs as compared to wild-type (WT) and empty vector (EV). TRAP activity was normalized to lysate protein concentration. **B,** TRAP activity, as measured by immunocytochemistry. Purple staining intensity indicates the activity level. The empty vector (**A**) and WT (**B**) are compared to $Thr^{5}Met$ (**C**), $Arg^{46}Trp$ (**D**), $Phe^{141}Val$ (**E**), $Thr^{183}Lys$ (**F**), $Val^{208}Met$ (**G**), $Glu^{213}Gln$ (**H**), $Met^{264}Lys$ (**I**), $Arg^{269}Trp$ (**J**), $Arg^{272}His$ (**K**), and $His^{282}Arg$ (**L**). Original magnification × 20. **C,** Western blot analysis. Concurrent with the PNPP assay shown in **A**, 10 μg of cell lysate and an equal volume of supernatant were analyzed by quantitative Western blotting using antihemagglutinin (aHA). Antitubulin (aTubulin) was used as a loading control in cell lysates and as quality control; its absence in supernatants indicates that supernatant proteins were secreted by intact cells. Results in **B** and **C** are representative of 4 independent experiments. **D,** PNPP activity in cell lysates and supernatants of 5 heterozygote variants plus WT as compared to empty vector plus WT and WT plus WT. Equal amounts of Strep-tagged WT and HA-tagged mutant *ACP5* were transfected. Expression of both constructs was confirmed by quantitative polymerase chain reaction analysis (data not shown). Values in **A** and **D** are the mean ± SEM of 4–6 independent experiments. $* = P < 0.05$ versus the corresponding WT or WT+WT group.

observed in 7 of them as compared to wild-type constructs (Figure 6A). This correlated well with the findings of cytochemical staining of transiently transfected homozygous HEK 293 cells (Figure 6B). Quantitative Western blotting demonstrated that protein levels were minimally altered in the lysate (Figure 6C), and a Pearson's correlation coefficient of TRAP expression to activity was low ($R^2 = 0.1$) (Supplementary Figure 5,

available online at http://onlinelibrary.wiley.com/doi/10.1002/art.39810/abstract). This suggests that only ~10% of the variation in activity in the lysate could be attributed to variation in the protein expression level. We therefore hypothesize that the origin of the majority of the variation in activity is not an absence of protein, but is due to an effect on catalytic activity. In contrast, in the supernatant, quantitative Western blotting demonstrated a reduction in protein levels in those variants in which activity levels were significantly reduced (Figure 6C). The high Pearson's correlation coefficient between relative TRAP expression and activity ($R^2 = 0.98$) (Supplementary Figure 5), suggests that >97% of the variation in activity can be attributed to variation in the protein expression level. As quality control in secretory pathways is highly efficient at sifting misfolded protein to ensure that only correctly folded active proteins are secreted, we propose that some variants may be misfolded and degraded, thus reducing secretion into the supernatant.

We cotransfected WT and mutant constructs for 5 of the SLE variants to more accurately simulate the heterozygous situation in SLE patients. We chose to express 4 variants that demonstrated significantly reduced activity in the homozygous state, in addition to the Thr^5Met variant for which in silico prediction was not possible since it lies outside of the reported crystal structure. Four of the SLE variants showed a reduction in TRAP activity, which was statistically significant in the lysate of 2 and the supernatant of 3 *ACP5* variant constructs (Figure 6D). While the activity of WT and mutant 1:1 cotransfections were reduced compared to WT plus WT, this reduction was not beyond that seen with WT plus empty vector, suggesting that this was not a dominant-negative effect. Western blot analysis was not possible in these cells due to the coexpression of WT and variant TRAP. However, equal expression of both constructs (WT plus mutant/WT plus empty vector) was confirmed by quantitative PCR. Of note, since shRNA knockdown of TRAP to ~33% expression was sufficient to cause ISG up-regulation following PDC stimulation (Figure 3D), we hypothesize that a number of these rare heterozygous *ACP5* missense variants are functionally and clinically relevant for lupus disease development due to reduced TRAP activity. Further assessments of subcellular localization and posttranslational processing may identify further functional consequences of point mutations, especially those that do not appear to affect protein activity.

DISCUSSION

In this study, we investigated the role of TRAP and OPN in innate immunity in humans, with special relevance to SPENCD and the systemic autoimmune disease SLE. We found that TRAP colocalized and physically interacted with OPN in PDCs and in macrophages and that OPN is a substrate for TRAP. When TRAP expression was reduced in PDCs, we observed that TLR-9 stimulation caused an increased nuclear translocation of *IRF7* and *NFKB*, with associated elevation of *IFNA*, ISGs, *IL6*, and *TNF* expression, thus offering an explanation for the IFN signature and inflammatory phenotype in SPENCD patients. Our findings may be of relevance not only to the pathogenesis of SPENCD, but also to lupus susceptibility, as in a survey of SLE patients, we demonstrated an overrepresentation of heterozygous *ACP5* missense variants, several of which displayed impaired catalytic activity.

To understand the relationship between TRAP deficiency and type I IFN production in SPENCD patients, the hypothesis that we explored in this study stems from the work of Shinohara et al (16), who reported that the association of OPN with the TLR-9/MyD88 signaling complex was essential for IFNα production in murine PDCs. However, in those studies, phosphorylation of OPN was not assessed. Activation of the TLR-9/MyD88 signaling pathway within PDCs has been shown to lead to both *IRF7* and *NFKB* nuclear translocation, resulting in the transcription of *IFNA*, *IL6*, and *TNF* (26). We established further evidence of a role of TRAP in the regulation of this pathway. Specifically, when we knocked down TRAP expression in a PDC line, we observed that TLR-9 stimulation caused increased nuclear translocation of both *IRF7* and *NFKB* along with an elevation in IFNα, IL-6, and TNF levels, as compared to control cell lines. These data are consistent with the clinical observation of significant elevation of IFNα in SPENCD cases (11) and elevated IL-6 levels detected in several patients.

We propose that the increased IFNα production following CpG-A stimulation in TRAP-deficient PDCs is secondary to the action of the persistent, unregulated activity of the TLR-9/MyD88/OPN signalosome, as illustrated in Figure 5D. Thus, TRAP deficiency would cause a lack of OPN dephosphorylation and deactivation, resulting in persistent formation of the OPN/TLR-9/MyD88 complex, with increased IFNα production and a predisposition to autoimmune disease. Unfortunately, we could not definitively confirm this possibility experimentally, as we were unable to assess OPN phosphorylation in PDCs by LC-MS/MS (due to limited substrate availability from even 50 million cells in our PDC-knockdown line). It therefore remains to be formally determined whether OPN is a physical component of the TLR-9/MyD88 complex in human immune cells or whether TRAP acts on a different, or even multiple, substrate(s) in this pathway.

The function of TRAP was previously explored in another myeloid-derived cell, the osteoclast. Ultrastructural immunohistochemistry revealed that, similar to OPN, TRAP is localized to the resorption lacuna, where it may directly contact bone OPN in an acidic environment (29). Here, TRAP dephosphorylation of OPN facilitated osteoclast migration during bone resorption (9). In TRAP-deficient mice, delayed clearance of the microbial pathogen *Staphylococcus aureus*, and a reduced population of macrophages in the peritoneal exudates was observed, suggesting that TRAP may directly or indirectly influence recruitment of macrophages to sites of microbial invasion (30). Concurrently, in vitro studies showed that phosphorylation-dependent interaction of OPN with its receptor regulated macrophage migration and activation (31). Whether TRAP regulation of OPN influences macrophage recruitment in SPENCD is yet to be determined.

It will be interesting to assess in further studies whether other potential TRAP substrates, including the additional possible interacting partners identified by the yeast 2-hybrid (if validated), may also be involved in the SPENCD phenotype, particularly relating to the observed increase in IL-6 and TNF levels.

Loss of TRAP activity causes SPENCD, and nearly half of all SPENCD patients fulfilled the ACR diagnostic criteria for SLE, while nearly all had positive titers of anti-dsDNA and/or ANA (11,12). These findings suggest that TRAP might influence susceptibility to idiopathic SLE. Sequencing of the *ACP5* gene in nearly 1,000 SLE patients demonstrated a significant excess of heterozygous *ACP5* missense variants in SLE patients compared to controls. In addition, using an in vitro transfection assay, we observed a reduction of TRAP activity with a number of the variants seen in SLE patients, indicating that impaired function of TRAP may play a role in the susceptibility to idiopathic lupus in a proportion of patients. The possibility that heterozygous *ACP5* variants may have pathogenic consequences is supported by the skeletal phenotype observed in the heterozygous ACP5-knockout mouse (13), and we also note a cellular phenotype was observed with a lentiviral TRAP knockdown of 67%.

In conclusion, our findings indicate that TRAP and OPN colocalize and that OPN is a substrate for TRAP in immune cells. Significantly, TRAP deficiency in PDCs leads to increased IFNα production, providing at least a partial explanation for how biallelic mutations in *ACP5* cause SLE in the context of SPENCD. Detection of heterozygous *ACP5* missense variants in lupus patients suggests that impaired function of TRAP may play a role in the susceptibility to idiopathic lupus.

ACKNOWLEDGMENTS

We thank Dr. Goran Andersson for kindly providing the TRAP antibody for confocal microscopy, Dr. Priska von Haller and Jimmy Eng for technical support with the mass spectrometry and bioinformatics support, Dr. Simon Lovell for performing the in silico assessments of the SLE genetic variants, and Drs. Xizhang Sun and Nalini Agrawal for technical support. We would also like to thank the Exome Aggregation Consortium (Cambridge, MA; online at http://exac.broadinstitute.org).

AUTHOR CONTRIBUTIONS

All authors were involved in drafting the article or revising it critically for important intellectual content, and all authors approved the final version to be published. Dr. Elkon had full access to all of the data in the study and takes responsibility for the integrity of the data and the accuracy of the data analysis.

Study conception and design. An, Briggs, Crow, Elkon.

Acquisition of data. An, Briggs, Dumax-Vorzet, Alarcón-Riquelme, Belot, Beresford, Bruce, Carvalho, Chaperot, Frostegård, Plumas, Rice, Vyse, Wiedeman, Crow, Elkon.

Analysis and interpretation of data. An, Briggs, Dumax-Vorzet, Crow, Elkon.

REFERENCES

1. Minkin C. Bone acid phosphatase: tartrate-resistant acid phosphatase as a marker of osteoclast function. Calcif Tissue Int 1982;34:285–90.
2. Hayman AR, Macary P, Lehner PJ, Cox TM. Tartrate-resistant acid phosphatase (Acp 5): identification in diverse human tissues and dendritic cells. J Histochem Cytochem 2001;49:675–84.
3. Hayman AR, Bune AJ, Bradley JR, Rashbass J, Cox TM. Osteoclastic tartrate-resistant acid phosphatase (Acp 5): its localization to dendritic cells and diverse murine tissues. J Histochem Cytochem 2000;48:219–28.
4. Chu P, Chao TY, Lin YF, Janckila AJ, Yam LT. Correlation between histomorphometric parameters of bone resorption and serum type 5b tartrate-resistant acid phosphatase in uremic patients on maintenance hemodialysis. Am J Kidney Dis 2003;41:1052–9.
5. Henriksen K, Tanko LB, Qvist P, Delmas PD, Christiansen C, Karsdal MA. Assessment of osteoclast number and function: application in the development of new and improved treatment modalities for bone diseases. Osteoporos Int 2007;18:681–5.
6. Rissanen JP, Suominen MI, Peng Z, Halleen JM. Secreted tartrate-resistant acid phosphatase 5b is a marker of osteoclast number in human osteoclast cultures and the rat ovariectomy model. Calcif Tissue Int 2008;82:108–15.
7. Janckila AJ, Yam LT. Biology and clinical significance of tartrate-resistant acid phosphatases: new perspectives on an old enzyme. Calcif Tissue Int 2009;85:465–83.
8. Hayman AR. Tartrate-resistant acid phosphatase (TRAP) and the osteoclast/immune cell dichotomy. Autoimmunity 2008;41:218–23.
9. Ek-Rylander B, Flores M, Wendel M, Heinegård D, Andersson G. Dephosphorylation of osteopontin and bone sialoprotein by osteoclastic tartrate-resistant acid phosphatase: modulation of osteoclast adhesion in vitro. J Biol Chem 1994;269:14853–6.
10. Inoue M, Shinohara ML. Intracellular osteopontin (iOPN) and immunity. Immunol Res 2011;49:160–72.
11. Briggs TA, Rice GI, Daly S, Urquhart J, Gornall H, Bader-Meunier B, et al. Tartrate-resistant acid phosphatase deficiency causes a bone dysplasia with autoimmunity and a type I interferon expression signature. Nat Genet 2011;43:127–31.
12. Lausch E, Janecke A, Bros M, Trojandt S, Alanay Y, de Laet C, et al. Genetic deficiency of tartrate-resistant acid phosphatase

associated with skeletal dysplasia, cerebral calcifications and autoimmunity. Nat Genet 2011;43:132–7.
13. Hayman AR, Jones SJ, Boyde A, Foster D, Colledge WH, Carlton MB, et al. Mice lacking tartrate-resistant acid phosphatase (Acp 5) have disrupted endochondral ossification and mild osteopetrosis. Development 1996;122:3151–62.
14. Patarca R, Saavedra RA, Cantor H. Molecular and cellular basis of genetic resistance to bacterial infection: the role of the early T-lymphocyte activation-1/osteopontin gene. Crit Rev Immunol 1993;13:225–46.
15. Trivedi T, Franek BS, Green SL, Kariuki SN, Kumabe M, Mikolaitis RA, et al. Osteopontin alleles are associated with clinical characteristics in systemic lupus erythematosus. J Biomed Biotechnol 2011; 2011:802581.
16. Shinohara ML, Lu L, Bu J, Werneck MB, Kobayashi KS, Glimcher LH, et al. Osteopontin expression is essential for interferon-α production by plasmacytoid dendritic cells. Nat Immunol 2006;7:498–506.
17. Lang P, Andersson G. Differential expression of monomeric and proteolytically processed forms of tartrate-resistant acid phosphatase in rat tissues. Cell Mol Life Sci 2005;62:905–18.
18. Tan EM, Cohen AS, Fries JF, Masi AT, McShane DJ, Rothfield NF, et al. The 1982 revised criteria for the classification of systemic lupus erythematosus. Arthritis Rheum 1982;25:1271–7.
19. Strater N, Jasper B, Scholte M, Krebs B, Duff AP, Langley DB, et al. Crystal structures of recombinant human purple acid phosphatase with and without an inhibitory conformation of the repression loop. J Mol Biol 2005;351:233–46.
20. Ljusberg J, Ek-Rylander B, Andersson G. Tartrate-resistant purple acid phosphatase is synthesized as a latent proenzyme and activated by cysteine proteinases. Biochem J 1999;343:63–9.
21. Andersson G, Ek-Rylander B, Hollberg K, Ljusberg-Sjolander J, Lang P, Norgard M, et al. TRACP as an osteopontin phosphatase. J Bone Miner Res 2003;18:1912–5.
22. Chaperot L, Bendriss N, Manches O, Gressin R, Maynadie M, Trimoreau F, et al. Identification of a leukemic counterpart of the plasmacytoid dendritic cells. Blood 2001;97:3210–7.
23. Liu Y, Shi Z, Silveira A, Liu J, Sawadogo M, Yang H, et al. Involvement of upstream stimulatory factors 1 and 2 in RANKL-induced transcription of tartrate-resistant acid phosphatase gene during osteoclast differentiation. J Biol Chem 2003;278:20603–11.
24. Christensen B, Klaning E, Nielsen MS, Andersen MH, Sorensen ES. C-terminal modification of osteopontin inhibits interaction with the $\alpha V\beta 3$-integrin. J Biol Chem 2012;287:3788–97.
25. Wang KX, Denhardt DT. Osteopontin: role in immune regulation and stress responses. Cytokine Growth Factor Rev 2008;19: 333–45.
26. Gilliet M, Cao W, Liu YJ. Plasmacytoid dendritic cells: sensing nucleic acids in viral infection and autoimmune diseases. Nat Rev Immunol 2008;8:594–606.
27. Briggs TA, Rice GI, Adib N, Ades L, Barete S, Baskar K, et al. Spondyloenchondrodysplasia due to mutations in ACP5: a comprehensive survey. J Clin Immunol 2016;36:220–34.
28. Rice GI, Kasher PR, Forte GM, Mannion NM, Greenwood SM, Szynkiewicz M, et al. Mutations in ADAR1 cause Aicardi-Goutières syndrome associated with a type I interferon signature. Nat Genet 2012;44:1243–8.
29. Flores ME, Norgard M, Heinegård D, Reinholt FP, Andersson G. RGD-directed attachment of isolated rat osteoclasts to osteopontin, bone sialoprotein, and fibronectin. Exp Cell Res 1992; 201:526–30.
30. Bune AJ, Hayman AR, Evans MJ, Cox TM. Mice lacking tartrate-resistant acid phosphatase (Acp 5) have disordered macrophage inflammatory responses and reduced clearance of the pathogen, Staphylococcus aureus. Immunology 2001;102: 103–13.
31. Weber GF, Zawaideh S, Hikita S, Kumar VA, Cantor H, Ashkar S. Phosphorylation-dependent interaction of osteopontin with its receptors regulates macrophage migration and activation. J Leukoc Biol 2002;72:752–61.
32. Ek-Rylander B, Andersson G. Osteoclast migration on phosphorylated osteopontin is regulated by endogenous tartrate-resistant acid phosphatase. Exp Cell Res 2010;316:443–51.